

Observation of Final-State Screening in Inverse Photoemission from Adsorbed Xenon Layers

K. Horn, K. H. Frank, and J. A. Wilder

Fritz-Haber-Institut der Max-Planck-Gesellschaft, D-1000 Berlin 33, Federal Republic of Germany

and

B. Reihl

IBM Zurich Research Laboratory, CH-8803 Rüschlikon, Switzerland

(Received 5 May 1986)

Inverse photoemission spectra of xenon layers adsorbed on Au(110) have been recorded. The unoccupied levels of xenon exhibit layer-dependent peak shifts to higher energies. The $6s$ level of the second xenon layer is shifted by 0.65 eV relative to the monolayer energy, with the $6p$ level exhibiting a 0.85-eV shift. These shifts are related to the image-charge screening of the negative-ion inverse-photoemission-spectra final states. This observation demonstrates the influence of screening in inverse photoemission, and provides a test of the different conflicting models put forward in explanation of such shifts.

PACS numbers: 73.20.Hb, 79.60.Gs

Rare-gas atoms provide ideal models for a study of the interaction of adsorbates and surfaces, and for an investigation of the relationship between the results of various spectroscopic probes and the ground-state properties of adsorbates in general.¹⁻³ Because of the weak interaction of these adsorbed layers with metal surfaces, any initial-state effects due to chemical interaction may be neglected; therefore the screening mechanisms important in the different electron spectroscopies may be studied directly. Here we employ inverse photoemission spectroscopy (IPS) to study such relaxation effects in the negative-ion final state of IPS in monolayers and multilayers of xenon adsorbed on Au(110).

IPS provides information on unoccupied electronic states^{4,5} and has so far been mostly applied to bulk and surface states of solids. However, some attention has been paid to adsorbates, in particular to adsorbed CO. The $2\pi^*$ level of CO on Ni, Pd, Cu, and Pt was studied by Himpsel and Fauster,⁶ and related to the differences in the chemisorption bond with these metals. Although the relation of the peak positions in the IP spectrum to ground-state one-electron energies has been discussed, to date there has been no clear experimental evidence of final-state effects in IPS.

This problem, well known from photoemission (PE),⁷ is often circumvented by the comparison of spectra with one-electron ground-state calculations. This comparison is misleading since it neglects the fact that the negative-ion final state in IPS is expected to be screened by the metal surface. A determination of this screening effect is therefore of importance for a proper interpretation of IPS adsorbate spectra.

Kaindl and co-workers have shown² that relaxation effects in photoemission may be analyzed through the observation of distance-dependent shifts in the line

positions of adsorbed rare-gas atoms, and that these shifts may be explained on the basis of a simple image-charge screening model. In order to ascertain whether this model is applicable to the IPS final state, we have recorded IP spectra of xenon on Au(110), and multilayer spectra of xenon on Ag(110) and Ag(100).⁸ We assign the IPS peaks through comparison of our data with transition energies between occupied and unoccupied levels in electron-energy-loss spectroscopy⁹ (EELS) and optical absorption¹⁰ (in which the adatom is excited but electrically neutral).

The experiments were carried out in a stainless steel chamber with a base pressure of 1×10^{-10} mbar, equipped with ion gun, LEED and Auger-electron spectroscopy facilities, an electrostatically focused electron gun with BaO cathode, and a photon detector consisting of a Geiger-Müller tube with a SrF₂ entrance window. In conjunction with iodine as a counting gas, this inverse photoemission apparatus detects photons of 9.5 eV energy with a resolution (electrons plus photons) of about 0.4 eV. The crystal was mounted on a specimen manipulator capable of cooling the sample to about 35 K by means of liquid helium. Cleaning of the crystal was accomplished by use of short cycles of argon-ion bombardment and annealing. Monolayer coverages of Xe were achieved by exposure of the crystal to 100 L Xe (1 L = 1×10^6 Torr-sec) at a crystal temperature of about 70 K, which is well above the desorption temperature for Xe multilayers. Second and higher layers were prepared by controlled exposures at about 35 K, with subsequent annealing to 60 K for 30 sec.

A series of IP spectra of the clean and xenon-covered Au(110) surface is shown in Fig. 1. The spectrum of the clean Au(110)(1×2) surface exhibits a surface state at 1.8 eV above E_F in agreement with

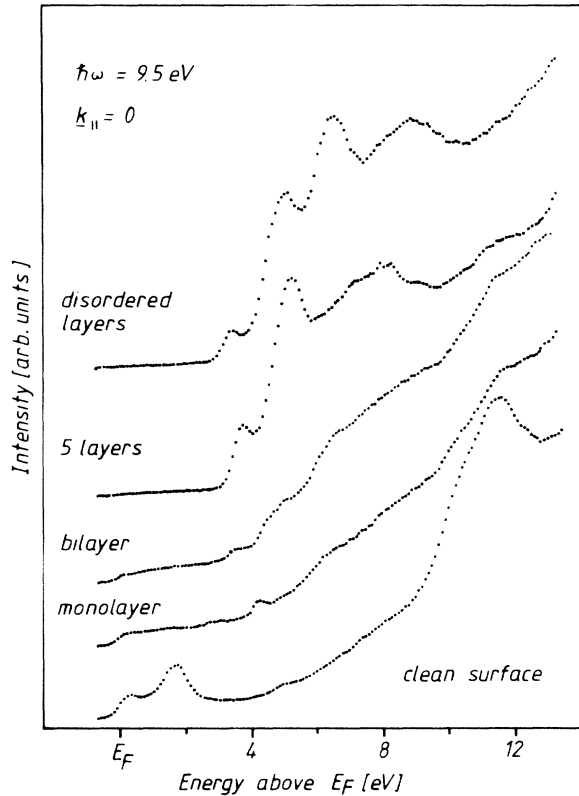


FIG. 1. Inverse photoemission spectra of clean and xenon-covered Au(110). Layer thickness is indicated in the figure. The disordered layer was produced by dosing of the crystal with xenon at a crystal temperature of 35 K, without subsequent annealing, and is approximately five layers thick.

earlier work,¹¹ weak emission from an image-potential feature at 4.8 eV above E_F , and strong peaks between 10 and 12 eV above E_F which are identified as transitions into final bands near the X point (X_6^- and X_7^- ; see Eckardt, Fritsche, and Noffke¹²). Upon monolayer coverage with xenon, these three features are strongly suppressed, and new peaks appear at 3.0 eV (weak), 4.25 eV (sharp), and about 6.4 eV (broad) above E_F (see Fig. 2, curve *a*, for an enlarged plot of this region). Upon exposure of the monolayer to further doses of xenon, both of the low-energy features (3.0 and 4.25 eV) are modified in a similar fashion. In both cases, the valleys to the high-energy side of the monolayer features are filled in with the first additional dose of xenon (Fig. 2, curve *b*). Both peaks are broadened, with the first peak developing a new maximum at about 3.3 eV above E_F . Figure 2, curve *c*, shows that, in fact, the new features are clearly defined with the next dose of xenon. These features are in the same position as the "filling in" evidenced in Fig. 2, curve *b*. The monolayer features remain distinct and unshifted as low-energy shoulders on the new features. The maximum of the first peak is now seen to be at 3.65 eV above E_F , with the second peak

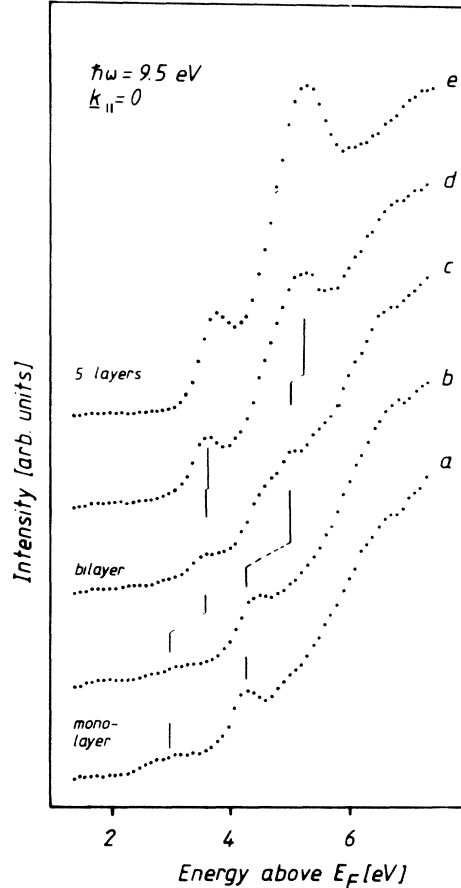


FIG. 2. Detail of the inverse photoemission spectra of xenon on Au(110) in the region of the 6s and 6p transitions: curve *a*, monolayer coverage; curve *b*, incomplete bilayer; curve *c*, complete bilayer; curve *d*, three layers; curve *e*, five layers.

at 5.05 eV above E_F . According to our coverage calibration, spectrum *b* corresponds to an incomplete double layer, and spectrum *c* to a complete double layer. The peak at 5.05 eV dominates upon subsequent exposures (three layers, Fig. 2, curve *d*, and five layers, Fig. 2, curve *e*), and the first peak is now clearly visible at 3.65 eV above E_F . In order to demonstrate the shift in the first and second peaks more clearly in Fig. 2, the shifts are indicated by lines connecting the peaks. The spectrum from a disordered, unannealed coverage is presented at the top of Fig. 1 in order to allow a comparison with features derived from the atomic states, and to evaluate any changes that may occur upon band formation in these unoccupied valence levels.

In EELS and optical-absorption measurements on rare-gas layers, resonant transitions from the occupied 5p to the unoccupied 6s, 6p, 5d, and higher states are observed.^{9,10} Thus we assign the peaks in the monolayer spectrum of Figs. 1 and 2 to the negative-ion analogs of these unoccupied states of the excited atom;

the peak at 3.0 eV to a transition into the $6s$ level and the peak at 4.25 eV to the $6p$ level. Features at higher energy, prominent in the multilayer spectra, are related to the higher s -, p -, and d -derived states as outlined below.

The assignment of the first peak as due to the $6s$ level is straightforward because of its position below the vacuum level, where the position of E_{vac} (4.88 eV above E_F) was derived from known work-function data¹³ for Au(110) and the work-function change induced by xenon adsorption.¹⁴ The $6p$ and higher states, however, are situated near or above the vacuum level, and it is therefore appropriate to identify these as resonances.

Consider now the layer-dependent shifts depicted in Fig. 2. The $6s$ peak of the double layer (Fig. 2, curve c) is shifted by 0.65 eV to higher energy, away from E_F , compared with the same feature in the monolayer. The second-layer $6p$ peak lies on the high-energy side of its monolayer peak, and is shifted by 0.85 eV. Spectrum c thus consists of a superposition of monolayer and second-layer peaks. We note that the peak intensity ratios in the monolayer (Fig. 2, curve a) and the five-layer (Fig. 2, curve e) spectra are nearly identical (about 2:1). Therefore, we are confident that the spectral features of the multilayers are identical to those of the monolayer, but shifted to *higher* energy above E_F .

We base our analysis of these shifts on two points. First, the monolayer-to-monolayer shifts are of similar magnitude to the shifts in peak position between monolayer and the disordered Xe layer (Fig. 1). Second, it has also been shown that bandwidth changes between the first and second layers¹⁵ are very small. These facts imply that the same physical process is taking place in both the ordered and disordered multilayers. Therefore, these shifts cannot be due to band formation in the second and higher layers, since the features in the disordered layers are related to the atomic levels. It is not surprising that the monolayer-derived features disappear upon further dosing with xenon (Figs. 2, curves d and e), since at this point, the number of overlayer adsorbate atoms is at least three times that of the monolayer population.

We interpret these shifts as being due to screening of the IPS final state by the image charge induced in the metal surface by the negative ion, with a screening energy depending on the distance z to the (image plane of the) surface according to

$$E_{\text{scr}} = -e^2/4z, \quad (1)$$

where e is the electronic charge. The effect of screening on IPS peak position may be visualized as follows: In an isolated atom, the additional electron in the negative-ion state experiences Coulomb repulsion from the electrons in the filled levels. In an atom

close to a metal surface, the extra electron induces a positive image charge in the metal, which binds the electron more strongly and therefore leads to an energy increase, i.e., the IPS peak appears closer to E_F than in the unscreened case. We emphasize that these are physisorbed layers; therefore the determination of the peak shifts between monolayer and multilayer coverage permits the analysis of this effect in the rare-gas layers without the interference of initial-state shifts resulting from charge transfer. In Fig. 2, the shift of the $6s$ level between monolayer and multilayer is 0.8 eV; similarly, the value for the $6p$ level is 1.0 eV.

It is instructive to compare these shifts with the analogous valence-level shifts observed in photoemission. Mandel *et al.*,¹⁶ in their study of layer-by-layer band structures of physisorbed xenon on Al(111), observe a shift of 0.50 eV between the first and second layers, with an overall shift of 0.82 eV for a three-layer coverage. Thus the shifts in the PE data compare favorably with those that we observe in IPS. Since the unoccupied levels probed in IP have a greater spatial extent, one might expect the screening effect to be smaller than for the occupied levels. This is not the case, and we defer a quantitative analysis of screening effects until further data, namely IPS studies of the other rare gases, are available. In addition, theoretical calculations concerning these systems are much needed.

The observation of the screening shifts allows us to clarify a controversy concerning the interpretation of layer-dependent valence-level shifts in rare-gas photoemission. Wandelt and co-workers^{15,17} have put forward an explanation of such shifts in terms of a "local work function" model. Here, it is assumed that the adsorbed xenon atom is situated sufficiently far outside the dipole layer of the metal surface that the Xe levels are pinned to the vacuum level in front of the adsorption sites. Hence the local work function at this specific site may be determined. Since the model is based on the assumption that the Xe levels are pinned to the vacuum level of the clean surface, the shift of the Xe peak position in the second layer is then due to the work-function change induced by the first layer. Since in photoemission, both the screening model and the "local work function" model predict shifts in the same direction, namely to higher binding energy, an unambiguous determination of the merits of the local-work-function model is hindered. The difficulty arises because the local-work-function model rests on the small differences between work-function change and screening-energy differences. In inverse photoemission, however, the two models predict opposite directions for the layer-dependent shift. Since the work function decreases upon xenon adsorption on metals,^{14,18} a pinning of the unoccupied Xe levels to the vacuum level, as presumed in the local-work-

function model, would result in the second-layer IPS peaks being shifted toward the Fermi level. This prediction is in disagreement with our results. Theoretical considerations show¹⁹ that the dipole due to the adsorbed Xe atom lies between the metal and the atom, such that its levels are pinned to the vacuum level of the Xe-covered surface, contrary to the assumptions of the local-work-function model. Thus while local work functions may be probed by photoemission from xenon, one must keep in mind that these are the local work functions of the *Xe-covered* surface.

Our final comment concerns the assignment of the peaks in the five-layer spectrum. In the disordered layer, we observe two additional peaks. By comparison with the EELS data,⁹ we assign these to transitions into the *5d* level (6.45 eV) and into a closely-spaced sequence of higher-lying levels (broad peak at 8.75 eV). This argument is supported by a comparison of the spectrum of the ordered layer with the conduction band structure calculated by Rössler.²⁰ The sharp *d* structure in the disordered layer is smeared out into a broad double peak at the position of the *d*-derived final bands in the calculation. We are at present not able to determine experimentally whether the peaks in the spectrum are due to *k*-conserving transitions or density-of-states features.

This work was supported in part by the Sonderforschungsbereich 6 der Deutschen Forschungsgemeinschaft. The authors would like to thank E.-E. Koch for constructive discussions and H.-P. Übel for his invaluable technical support. One of us (K.H.) would like to thank IBM Zurich for their hospitality and support in the initial stages of this work.

¹*Ordering in Two Dimensions*, edited by S. K. Sinha

(North-Holland, New York, 1980).

²G. Kaindl, T.-C. Chiang, D. E. Eastman, and F. J. Himpsel, Phys. Rev. Lett. **45**, 1808 (1980).

³K. Horn, A. M. Bradshaw, and M. Scheffler, Phys. Rev. Lett. **41**, 822 (1978).

⁴V. Dose, Prog. Surf. Sci. **13**, 225 (1983).

⁵B. Reihl, Surf. Sci. **162**, 1 (1985); F. J. Himpsel, Comments Solid State Phys. (to be published).

⁶F. J. Himpsel and Th. Fauster, Phys. Rev. Lett. **49**, 1583 (1982); P. D. Johnson, D. A. Wesner, J. W. Davenport, and N. V. Smith, Phys. Rev. B **30**, 4860 (1984); J. Rogozik, V. Dose, K. C. Prince, A. M. Bradshaw, P. S. Bagus, K. Hermann, and Ph. Avouris, Phys. Rev. B **32**, 4269 (1985); S. Ferrer, K. H. Frank, and B. Reihl, Surf. Sci. **162**, 264 (1985).

⁷H. Siegbahn and L. Karlsson, in *Encyclopedia of Physics*, edited by W. Mehlhorn (Springer-Verlag, Berlin, 1982).

⁸B. Reihl, K. H. Frank, and K. Horn, to be published.

⁹J. E. Demuth, Ph. Avouris, and D. Schmeisser, Phys. Rev. Lett. **50**, 600 (1983).

¹⁰G. Schönhense, A. Eyers, and U. Heinzmann, Phys. Rev. Lett. **56**, 512 (1986).

¹¹G. Binnig, K. H. Frank, H. Fuchs, N. Garcia, B. Reihl, H. Rohrer, F. Salvan, and A. R. Williams, Phys. Rev. Lett. **55**, 991 (1985).

¹²H. Eckardt, L. Fritsche, and J. Noffke, J. Phys. F **14**, 97 (1984).

¹³H. C. Potter and J. M. Blakely, J. Vac. Sci. Technol. **12**, 635 (1975).

¹⁴G. McElhiney and J. Pritchard, Surf. Sci. **60**, 397 (1976).

¹⁵R. Miranda, E. V. Albano, S. Daiser, G. Ertl, and K. Wandelt, Phys. Rev. Lett. **51**, 782 (1983).

¹⁶T. Mandel, G. Kaindl, M. Domke, W. Fischer, and W. D. Schneider, Phys. Rev. Lett. **55**, 1638 (1985).

¹⁷R. Miranda, S. Daiser, K. Wandelt, and G. Ertl, Surf. Sci. **131**, 61 (1983).

¹⁸S.-I. Ishi and Y. Ohno, Surf. Sci. **159**, L401 (1983).

¹⁹N. D. Lang, Phys. Rev. Lett. **46**, 842 (1981).

²⁰U. Rössler, Phys. Status Solidi (B) **45**, 483 (1971).